Published in final edited form as:
Contrast Media Mol Imaging. 2011 ; 6(4): 189–199. doi:10.1002/cmmi.417.

Surface Functionalization of Magnetic Iron Oxide Nanoparticles for MRI Applications – Effect of Anchoring Group and Ligand Exchange Protocol

Eric D. Smolensky[a], **Hee-Yun E. Park**[a], **Thelma S. Berquó**[a], and **Valérie C. Pierre**[a,*]
[a]Department of Chemistry, 207 Pleasant Street SE, University of Minnesota, Minneapolis, MN 55455, USA

Abstract

Hydrophobic magnetite nanoparticles synthesized from thermal decomposition of iron salts must be rendered hydrophilic for their application as MRI contrast agents. This process requires refunctionalizing the surface of the nanoparticles with a hydrophilic organic coating such as polyethylene glycol. Two parameters were found to influence the magnetic behavior and relaxivity of the resulting hydrophilic iron oxide nanoparticles: the functionality of the anchoring group and the protocol followed for the functionalization. Nanoparticles coated with PEGs via a catecholate-type anchoring moiety maintain the saturation magnetization and relaxivity of the hydrophobic magnetite precursor. Other anchoring functionalities, such as phosphonate, carboxylate, and dopamine decrease the magnetization and relaxivity of the contrast agent. The protocol for functionalizing the nanoparticles also influences the magnetic behavior of the material. Nanoparticles refunctionalized according to a direct biphasic protocol exhibit higher relaxivity than those refunctionalized according to a two-step procedure which first involves stripping the nanoparticles. This research presents the first systematic study of both the binding moiety and the functionalization protocol on the relaxivity and magnetization of water-soluble coated iron oxide nanoparticles used as MRI contrast agents.

Keywords

MRI; contrast agent; MION; iron oxide nanoparticles; superparamagnetic agents; surface functionalization; relaxivity; magnetism

Introduction

Due to their superparamagnetic behavior, iron oxide nanoparticles received significant attention over the last few decades as contrast agents for magnetic resonance imaging (1–3). When compared to their paramagnetic, gadolinium-based counterparts, iron oxide nanoparticles have similar longitudinal relaxivities, r_1, but more powerful transverse relaxivities, r_2, at the field of clinical relevance (> 10 MHz). For instance, the longitudinal and transverse relaxivities of the particulate contrast agent Sinerem® (Guerbet, France) are 22.7 $mM_{Fe}^{-1}s^{-1}$ and 53.1 $mM_{Fe}^{-1}s^{-1}$ at 20 MHz and 37 °C, respectively (4,5). Comparatively, the relaxivities of Gd-DTPA (Magnevist®, Schering A.G., Germany) are 3.4 $mM^{-1}s^{-1}$ and 4.0 $mM^{-1}s^{-1}$.(6, 36) However, in contrast to gadolinium complexes, the parameters influencing the efficacy of iron oxide nanoparticles are poorly understood. In the case of gadolinium complexes, the Solomon-Bloembergen-Morgan equation, which relates

*Correspondence: V. C. Pierre, Department of Chemistry, University of Minnesota, Minneapolis, MN 55455, USA. pierre@umn.edu.

the influence of the number of coordinated water molecules, their exchange rate, the electronic relaxation time of the metal, and the rotational correlation time of the complex to its longitudinal relaxivity, is now well-established (7–10) In the case of particulate contrast agents, the different parameters influencing the longitudinal and transverse relaxivities and the correlations between these parameters are not as well understood. The importance of the intrinsic properties of the nanoparticles, such as their phase, size, shape, and crystallinity, on their magnetic behavior are starting to be elucidated (4,9–17). However, much debate still exists over how each of these variables affects properties such as surface spin canting and magnetic anisotropy and, consequently, the relaxivities of the contrast agents.

One additional parameter that has received little attention is the nature of the organic coating and in particular the nature of its anchoring group (18). Because of their poor solubility and stability in water at physiological pH iron oxide nanoparticles used in biomedical applications need to be coated with a water soluble polymer. However, in many biological investigations, it is often assumed that the nature of this coating, and the procedure followed to anchor it on the surface of the nanoparticles have little effect on the magnetic properties and relaxivity of the particulate contrast agents. This assumption, however, proves to be far from true. Recent reports have demonstrated that refunctionalization of magnetite and maghemite nanoparticles with sulfonates,(19) phosphonates,(19,20) carboxylates,(21) or silicates (22) can significantly reduce their magnetization. Similarly, despite an earlier report,(23) dopamine was recently shown to react with iron oxide nanoparticles (24). Herein, we present a systematic study of the influence of the surfactant's anchoring group and the refunctionalization protocol on the magnetic properties and relaxivities of magnetite nanoparticles.

The synthesis of iron oxide nanoparticles of controlled size, shape, and phase have recently been reported by Sun (25) and Hyeon (16) among others. These methods typically involve the thermal decomposition of iron complexes in the presence of surfactants and produce nanoparticles significantly more monodisperse than those synthesized by co-precipitation of Fe(II) and Fe(III) salts in basic aqueous solutions (26). Additionally, nanoparticles synthesized according to these protocols exhibit higher structural similarities and improved magnetic properties when compared to those produced by the coprecipitation methods. Concomitant with the synthesis of the monodisperse nanoparticles is their coating with the hydrophobic surfactants oleic acid and oleylamine. Biological applications, however, require that the nanoparticles be stable in water at physiological pH, which in turn requires that the hydrophobic coating be replaced by a hydrophilic one. This is commonly done by either of two protocols: stripping of the oleic acid coating in ethanol followed by refunctionalization with a hydrophilic ligand, or direct biphasic replacement of oleic acid by a ligand which has higher affinity for iron (Scheme 1). The effect of these synthetic procedures on the resulting magnetic properties and relaxivities of the nanoparticles has not been studied.

To explore the influence of the anchoring group of the solubilizing ligand and the protocol for surface functionalization on the efficacy of Magnetic Iron Oxide Nanoparticles (MION) contrast agents, monodisperse magnetite nanoparticles were refunctionalized with a library of discrete PEGs terminated with various chelators, and their magnetic properties and relaxivities were measured. Four different chelators were chosen for this study due to their widespread use as capping agents in the literature: catechol, 2,3-dihydroxybenzamide, phosphonic acid, and carboxylic acid (Chart 1) (19,20,23,27). Since dopamine was previously shown to react with iron oxide nanoparticles (24), dopamine-functionalized MION were also studied. Water-dispersable soap-covered magnetite nanoparticles were used as control, as their synthesis does not involve invasive replacement of the original oleic acid coating.

Experimental Methods

General

Unless otherwise noted, starting materials were obtained from commercial suppliers and used without further purification. Discrete PEG was purchased from Quanta Biodesign. HPLC chromatograms were obtained from a Varian Prostar HPLC using acetonitrile/water gradients and a Varian Dynamax C18 semipreparative column. ^{1}H-NMR spectra were recorded on a Varian 500 at 500 MHz or on a Varian 300 at 300MHz; the solvent residual peak was used as an internal reference. Data for ^{1}H NMR are recorded as follows: chemical shift (δ, ppm), multiplicity (s, singlet; d, doublet; t, triplet, m, multiplet; dd, doublet of doublets), integration, coupling constant. Mass spectra were recorded on a Bruker BioTOF II ESI-MS. TEM images were collected on a JOEL JEM1210, FEI Tecnai T12, and on a JOEL 1200 EXII at 120 kV. Magnetic data (ZFC/FC magnetization curves and hysteresis plots) were recorded on a commercial SQUID magnetometer (MPMS-XL - Quantum Design). The saturation magnetization value are given after extraction of the weight contribution of the organic part. Powder X-ray diffraction (XRD) was performed using a PANalytical X-Pert PRO MPD X-ray diffractometer equipped with a cobalt source and an X-Celerator detector. Data was collected over the range of 10–90° 2θ at a scan rate of 0.6° per minute. The diffraction patterns were compared to the reference powder diffraction files (PDF) for magnetite (#19–629). The ZFC/FC curves were obtained in an applied magnetic field (H = 5 mT) and performed while heating the sample in the range 10<T<170 K in zero-field-cooled (ZFC) and field-cooled (FC) procedures using a commercial SQUID magnetometer (MPMS-XL - Quantum Design). Hysteresis loops were obtained at 10 K by using maximum applied fields up to 1 T in field cooling treatment. Elemental analysis by Inductively Coupled Plasma Optical Emission Spectroscopy (ICP-OES) on a Perkin-Elmer Optima 3000V was performed by the Soil Testing and Research Analytical Laboratory of the University of Minnesota, Twin-Cities. Prior to analysis by ICP, all nanoparticles samples were digested in concentrated nitric acid at 100° C overnight.

DHB-PEG (1)—2,3-Dihydroxybenzoic acid (40 mg, 0.26 mmol) and HATU (2-(7-Aza-1H-benzotriazole-1-yl)-1,1,3,3-tetramethyluronium hexafluorophosphate) (110 mg, 0.28 mmol) were dissolved in anhydrous dimethylacetamide (DMA), (5 mL). The clear solution was stirred at room temperature for 15 min. 2,5,8,11,14,17,20,23-octaoxapentacosan-25-amine (m-dPEG8-amine) (85 mg, 0.26 mmol) followed by N-diisopropylethylamine (67 mg, 0.52 mmol) were subsequently added. The reaction mixture turned yellow immediately and was stirred overnight at room temperature. The crude product was purified by HPLC and fractions containing product lyophilized yielding (**1**) as a white solid (0.28 mg, 28 %). ^{1}H NMR (CD_3CN) δ = 7.12 (d, 1H, *J* = 7.0), 6.95 (d, 1H, *J* = 7.0), 6.76 (t, 1H, *J* = 6), 3.56 (t, 1H, *J* = 1.2), 3.53 (m, 30H), 3.29 (s, 1H). ES-MS *m*/*z* (relative intensity) 559.9 (11 %), 543.9 (100 %), 521.0 (3 %).

Dopamine-PEG (2)—Dopamine (52 mg, 0.22 mmol) and HATU (92 mg, 0.24 mmol) were dissolved in DMA (2 mL). The clear solution was stirred at room temperature for 15 min. Subsequently, 2,5,8,11,14,17,20,23-octaoxahexacosan-26oic acid (m-dPEG8-acid) (85 mg, 0.22 mmol) was added followed by N-diisopropylamine (56 mg, 0.44 mmol). The reaction mixture turned yellow immediately and then became colorless. The solution was stirred at room temperature overnight. A white precipitate was filtered and the mixture was purified by HPLC (gradient from 100 % water to 60 % acetonitrile over 1 h) and fractions containing the product were lyophilized. Dopamine (**2**) was obtained as a white solid (166 mg, 94%). ^{1}H NMR (CD_3CN) δ = 6.72 (d, 1H, *J* = 7.5), 6.68 (s, 1H); 6.56 (d, 1H, *J* = 6.6), 3.62 (d, 1H, *J* = 1.8), 3.55 (m, 30H), 3.46 (m, 2H), 3.3 (m, 5H), 2.6 (t, 2H, *J* = 4.8), 2.31 (t, 2H, J = 4.8). ES-MS *m*/*z* (relative intensity) 586.3 (28 %), 570.3 (100 %), 548.3 (10 %).

Diethylether-PO_4-PEG (3)—3-(Diethylphosphono) propanoic acid (26 mg, 0.13 mmol) and HATU (54 mg, 0.14 mmol) were dissolved in anhydrous DMF (5 mL). The clear solution was stirred at room temperature for 15 min. M-dPEG8-amine (99 mg, 0.26 mmol) followed by N-diisopropylethylamine (33 mg, 0.58 mmol) were subsequently added. The reaction mixture turned yellow immediately and then became colorless. The solution was stirred at room temperature overnight. The crude product was purified by flash chromatography over silica eluting with a gradient of 100 % CH_2Cl_2 to 92 % CH_2Cl_2 / 8% MeOH yielding (**3**) as a yellow oil (63 mg, 86 %). ^{1}H NMR (CD_3OD) δ = 4.11 (m, 4H), 3.64 (m, 32H); 3.36 (s, 3H), 2.46 (m, 2H), 2.09 (m, 2H), 1.34 (m, 6H). ES-MS *m*/*z* (relative intensity) 598.2 (100 %), 576.3 (42 %).

PO_4-PEG(4)—Dichloromethane (5 mL) was purged with N_2 for 30 min. Dry diethylether-PO_4-PEG (**3**) was added to the reaction solution followed by trimethylsilylbromide (222 mg, 4 eq.) The solution was stirred at room temperature overnight. The solvent was removed under vacuum and methanol/water (2:1) was added and the solution stirred at room temperature for 2 h. The product (**4**), was > 95 % by ^{1}H NMR and was used without further purification (133 mg, 77 %). ^{1}H NMR ($CDCl_3$) δ = 3.67 (m, 32H), 3.39 (s, 3H), 2.95 (m, 2H), 2.26 (m, 2H). ES-MS *m*/*z* (relative intensity) 542.3 (9 %) 520.4 (100 %).

Oleic acid-functionalized magnetite nanoparticles—Oleic-acid functionalized magnetite nanoparticles were synthesized from $Fe(acac)_3$, oleic acid and oleylamine according to the procedure developed by Wang and coworkers (25). Importantly, due to small variations in size and magnetic properties between different batches of synthesized magnetite nanoparticles, *all* functionalized nanoparticles discussed hereafter in this paper were prepared from this one batch of oleic-acid coated magnetite nanoparticles.

Soap-functionalization—Oleic acid coated nanoparticles (10 mg) and hexadecyltrimethylammonium bromide (10 mg) were suspended in chloroform (5 mL) and the black mixture was stirred overnight. The solvent was removed under reduced pressure and the resulting brown solid re-suspended in mQ water.

Refunctionalization of iron oxide nanoparticles was performed according to either of the following two protocols:

Surface Functionalization Protocol #1 – Two-step Exchange Protocol (Stripping Protocol): Iron oxide nanoparticles (10 mg) were suspended in chloroform (5 mL). Ethanol (10 mL) was added and the suspension centrifuged (5 min, 5000 rpm). The black pellet was collected, resuspended in ethanol (5 mL), and sonicated (< 20 sec). The suspension was centrifuged again (5 min, 5000 rpm) and the particles collected. The centrifugation-sonication process was repeated two more times resulting in stripped iron oxide nanoparticles (2–3 mg). The stripped nanoparticles were then added to a solution of surfactant **a–g** (Chart 1) in dichloromethane (5 mL) in a 1:1 mass ratio. The monophasic mixture was sonicated (10 min) and water (5 mL) was added. The mixture was then centrifuged (5 min, 13000 rpm) and the black-brown solid collected. Water (5 mL) was added and the centrifugation-wash procedure was repeated two more times. The resultant particles were suspended in water.

Surface Functionalization Protocol # 2 – Direct, Biphasic Protocol: Iron oxide nanoparticles (2–3 mg) were suspended in 10 mL of hexanes. This suspension was added to a methanol/water solution (2:5 ratio CH_3OH:H_2O, 7 mL, pH = 4) of the surfactant **a–g** (5 mg, Chart 1), and the resulting biphasic mixture sonicated for 1 h. The black aqueous phase

was separated and extracted with hexanes (3 × 20 mL). The aqueous phase was collected and lyophilized and the resulting black-brown nanoparticles were suspended in water.

Relaxivity—Longitudinal (T_1) and transverse (T_2) relaxation times of solutions of MION in mQ water were measured at 20° C on a Varian 300 at 300 MHz using the inverse recovery sequence and the Carr-Purcell-Meiboom-Gill sequence, respectively. The total concentration of iron of each sample was measured by ICP-OES following digestion of the nanoparticles by nitric acid. For each sample, T1 and T2 relaxation times were measured for four solutions of different nanoparticle concentrations. The longitudinal (r_1) and transverse (r_2) relaxivities were fitted to the following equation.

$$R_i[\mathrm{Fe}] = \frac{1}{T_{i,\mathrm{obs}}} - \frac{1}{T_{i,\mathrm{H_2O}}}, \text{ where } i = 1, 2$$

Results and Discussion

Oleic-Acid Functionalized Magnetite Nanoparticles

The magnetic properties and relaxivities of iron oxide nanoparticles are dependent both on the composition and size of the nanoparticles. For the purpose of this study, and in order to fully understand the effect of the coating on the magnetic property of the nanoparticles, it is imperative to use nanoparticles of controlled phase, size, and polydispersity. Magnetite nanoparticles were synthesized according to the method of Wang (25) via the controlled thermal decomposition of $Fe(acac)_3$ in the presence of oleic acid and oleylamine. The resulting nanoparticles were monodisperse, and mostly cubic in shape of size 7.1 ± 1.4 nm as measured by TEM (Figure 1a). It should be noted that by TEM, only the size of the core can be imaged. The thickness of the organic coating cannot be imaged directly by this technique. Thus, all particle size discussed hereforth are only relating to the size of the iron oxide core. As can be seen in the TEM image, an interparticle spacing of ca. 2 nm is maintained due to the hydrophobic interactions of oleic acid and oleylamine coating on the surface. Presence of the oleic acid was further established by FT-IR (Figure 2a and b). Analysis of the nanoparticles by powder XRD (Figure 3a) indicates that the observed diffraction pattern is in good agreement with published data for magnetite (JCPDS #19–629). Due to the strong similarity between the pattern of maghemite (γ-Fe_2O_3) and magnetite (Fe_3O_4), as well as significant line broadening due to the small size of the nanoparticles, the two phases cannot be distinguished solely from the XRD pattern. However, the calculated lattice parameter of 8.40(2) Å is in good agreement with the value of 8.38(2) Å for magnetite (JCPDS #19–629), and therefore strongly suggests that the nanoparticles are composed of Fe_3O_4. The size of the oleic acid coated particles, as calculated from the Scherrer equation (28) is 8.6 nm. It is in good agreement from the size calculated from the TEM images, suggesting that each particle exists as a single crystal.

The ZFC curve indicates that the oleic acid covered nanoparticles have a blocking temperature of 34 K (Figure 4). Furthermore, below the blocking temperature, the FC curve continues to increase in magnetization with decreasing temperature (Figure S1 in supporting information). This feature suggests that the particles are magnetically non-interacting. As expected, the hysteresis loop of the as-synthesized nanoparticles, measured below their blocking temperature at 10 K, presents a small coercivity of 0.013 Am^2/kg and a remanence of 16 Am^2/kg (Figure 5). The saturation magnetization of the nanoparticles is 49 Am^2/kg.

Soap-Covered Magnetite Nanoparticles

This study aims at understanding the effect of the anchoring group of the organic coating on the magnetic properties and relaxivities of particulate contrast agents. Relaxivity, a measure of the increase in relaxation rate of water protons imparted by the contrast agent, is only relevant if measured in aqueous solutions. The oleic acid coating of the as-synthesized magnetite, while effective at preventing particle aggregation, limits particle dispersion to organic solvents. Hence, the relaxivity of the as-synthesized nanoparticles cannot be measured. In order to have a control for our study, the oleic acid covered nanoparticles must be rendered hydrophilic without displacing the original oleic acid coating. This is best achieved by covering the nanoparticles with a second layer of surfactants such as N,N,N-trimethylhexadecan-1-ammonium. The long alkyl chain of this soap penetrates the nonpolar coating and intertwines with the greasy chain of the oleic acid (Chart 1b). The exposed ammonium group provides a shell of positive charge around the nanoparticles, thus rendering them water soluble. The soap covered nanoparticles therefore have two important structural features. First, the original oleic acid coating is not removed from the surface of the nanoparticles, such that this surface modification has minimal impact on the magnetic property of the nanoparticles. Second, a hydrophobic shell is maintained between the outermost ammonium and the metallic surface of the nanoparticles, thereby limiting the diffusion of water to the iron oxide surface. It is noteworthy that experiments in which excess oleic acid was added to form an analogous oleic acid bilayer failed to produce water-dispersible nanoparticles.

Addition of a layer of greasy ammonium on the nanoparticles is apparent from the FT-IR spectra of the functionalized nanoparticles. Two medium bands at 910 cm^{-1} and 960 cm^{-1}, characteristic of the ammonium soap, (Figure 2c) are also present in the spectrum of the soap covered nanoparticles (Figure 2d) but were not present in the as-synthesized oleic acid covered nanoparticles (Figure 2b). Importantly, as is evident from the TEM image (Figure 8a, Table 1) addition of this second hydrophilic group does not alter the shape or size of the particles.

The magnetic properties of the nanoparticles are affected by this extra coating of alkyl ammonium (Table 2). The blocking temperature increases from 34 K from the oleic-acid coated MION to 44 K for the soap covered particles (Figure 4). The nanoparticles maintain their superparamagnetic character, although their saturation magnetization increases significantly from 49 Am^2/kg to 71 Am^2/kg (Figure 5). Importantly, the extra soap coating renders the nanoparticles significantly water soluble, enabling the measurement of their relaxivity. At 300 MHz (7.0 T) and 20° C, the soap covered magnetite display minimal longitudinal relaxivity, but outstanding transverse relaxivity of 135 $mM_{Fe}^{-1}s^{-1}$, which is higher than the commercial USPIO Sinerem® (Guerbet, r_2 = 53.1 $mM_{Fe}^{-1}s^{-1}$) (5). It should be noted that the transverse relaxivity is mostly independent of the strength of the magnetic field (data not shown), whereas the longitudinal relaxivity increases substantially at lower magnetic fields (Figure 10). At 20 MHz and 20° C, r_1 of the soap-covered nanoparticles is 13.4 $mM_{Fe}^{-1}s^{-1}$, which is comparable to that of Sinerem® (r_1 = 22.7 $mM^{-1}s^{-1}$) (5). The difference between the relaxivities of the soap-covered magnetite and those of Sinerem® likely stems from the difference in size of the magnetite crystals (the mean crystal diameter of Sinerem® is 4.3–4.9 nm) and the procedure for their synthesis (29).

Surface Functionalization of Iron Oxide Nanoparticles

Although addition of a second layer of charged surfactant significantly increases the water solubility of the nanoparticles, the resulting contrast agents have two main disadvantages. First and foremost, the ammonium soap and the oleic acid can be removed under physiological conditions by phosphates naturally present in the blood; second, the greasy

oleic acid does not lend itself easily to functionalization with, for instance, targeting vectors. It is therefore beneficial to replace the oleic acid coating with a hydrophilic ligand that has higher affinity for iron oxide.

The oleic acid coating of the as-synthesized nanoparticles is usually replaced by a more hydrophilic one according to either of two protocols (Scheme 1): stripping of the oleic acid in ethanol followed by refunctionalization with an organic ligand (stripping protocol), or direct, biphasic exchange with a water soluble ligand that has higher affinity for iron than oleic acid (biphasic protocol). The stripping protocol enables substitution of the oleic acid coating with any organic ligand whether or not the latter is a strong chelator of iron. The biphasic protocol, on the other hand, relies on the lability of the oleate coating and on the affinity of the competing chelate for Fe(II) and Fe(III) relative to that of oleate. It is therefore only applicable to organic ligands whose anchoring group forms more stable iron complexes than carboxylates, such as catecholates, salicylates, phosphates, or phosphonates.

The hydrophilic ligands chosen for this study (Chart 1) have two distinct features: a chelating head and a water soluble tail. In this study, only the chelating head of each ligand varies; in each case the tail is composed of discrete polyethylene glycol oligomer (n=8). Four different chelating heads were studied: catechol, 2,3-dihydroxybenzamide, phosphonic acid, and carboxylic acid. Each ligand was synthesized by standard amide coupling conditions starting with either an acid or an amine terminated discrete PEG and purified by flash chromatography over silica or reverse phase HPLC. All ligands are pure and have correct analysis by NMR and mass-spectroscopy. Dopamine was also studied due to its reported ability to react with iron oxide nanoparticles (24).

As mentioned previously, refunctionalization of iron oxide nanoparticles coated with oleic acid can be performed according to either a stripping or a biphasic protocol. The stripping protocol requires two steps. First, the oleic acid ligands are stripped from the surface of the magnetite by brief sonication in ethanol, after which the nanoparticles are recovered by centrifugation. Repeating this sonication/centrifugation steps three times ensures that the majority of the oleic acid is removed, as evidenced from the lack of any oleic acid band in the FT-IR spectra of the naked nanoparticles (Figure 2e). Refunctionalization is then achieved by sonicating the naked nanoparticles in dichloromethane in the presence of the new hydrophilic ligand. Successful coating of the nanoparticles with the desired ligand is best characterized by FT-IR (Figure 2). In each case, bands corresponding to the ligand are also observed in the spectrum of the nanoparticles coated with that ligand. For instance, strong alkyl C-H stretching bands (2917 cm^{-1} and 2850 cm^{-1}) along with strong symmetrical and antisymmetrical C-O-vibration modes (1555 cm^{-1}), both of which originate from the oleic acid coating, are observed in oleic acid-MION (Figure 2b). When the particles are refunctionalized with any of the PEG ligands, distinct changes in the IR spectrum occur. Most apparent is the loss of the sharp C-H stretching bands and growth of broad C-H stretching bands. This is resultant from the loss of order in the capping ligands. Oleic acid, being an 18-chain hydrocarbon, forms well-defined monolayers on the nanoparticle surface; an interaction maintained by the hydrophobic and non-polar interactions of the hydrocarbon chain. PEG ligands, however, do not allow for such a well-defined layer as the molecules exist in a greater variety of conformations. Additionally, functionalization was further supported by the disappearance of C=O stretching and growth of peaks related to the bound functional molecule. Most prominent is the strong increase in C-O stretching at 1110 cm^{-1}. It is noteworthy that due to limitations of the IR spectrophotometer, Fe-O stretching band analysis was not obtainable.

The important aspect of this stripping method is the isolation of naked (uncoated) particles prior to their refunctionalization. This procedure therefore has the advantage that the oleic

acid can be replaced with any ligand, regardless of the latter's affinity for iron. Unfortunately, any modification to the nanoparticles, such as surface oxidation or agglomeration, that takes place either during the stripping or the isolation of the magnetite is irreversible. This change will manifest itself in the resultant magnetic properties and relaxivity of the material. Particle size and phase changes do occur during this synthesis, and is evident from both the TEM images and XRD data. As is apparent in the TEM image of the naked magnetite (Figure 1b), stripping the nanoparticles results in a significant increase in their polydispersity. Some nanoparticles are partially dissolved and become smaller, while others aggregate. As a result, even though the average diameter of the particles does not vary, the polydispersity increases from 1.4 nm for the oleic acid coated nanoparticles, to 2.0 nm for the naked nanoparticles. These particles maintain their polydispersity when they are coated with the PEG ligand. Notably, the increase in polydispersity observed while refunctionalizing the nanoparticles via this protocol is prominent for every ligand studied (Figure 6).

Moreover, while the powder XRD pattern does not change upon stripping, the decrease of 0.02 Å in the lattice parameter between the oleic acid coated and the naked nanoparticles suggests surface oxidation. This partial oxidation may be responsible for the decreased relaxivity observed for the corresponding nanoparticles. It should be noted that this procedure yields little refunctionalized material. Indeed, most stripped nanoparticles do not resuspend in water, even in the presence of a large excess of the hydrophilic ligand and with lengthy sonication time. Therefore, not enough material could be isolated to fully characterize the water soluble nanoparticles by XRD and magnetic measurements.

The biphasic, or direct exchange refunctionalization protocol, on the other hand, gives significantly higher yield of PEG coated nanoparticles. In this protocol, the initial oleic acid coated particles are suspended in an organic phase such as hexanes. The hydrophilic competing ligand is instead dissolved in the aqueous phase at basic pH (Figure 7 left). Since the oleic acid coating is labile, and since the competing ligand has higher affinity for iron than the oleic acid, sonication of the biphasic mixture enables the direct substitution of oleic acid by the competing ligand. As a result, the nanoparticles, now coated with hydrophilic ligands, transfer to the aqueous phase while the oleic acid remains in the organic phase (Figure 7 right). While this is an attractively simple procedure, it cannot be applied to every ligand. For instance, carboxylic acid terminated PEG have similar affinity for iron than oleic acid. Expectedly, the biphasic procedure failed to produce any CO_2-PEG-MION.

Advantageously, this procedure readily enables refunctionalization of most nanoparticles, and little material is lost during the synthesis. FT-IR spectroscopy confirms successful coating of the nanoparticles (Figure 2), but it should be noted that it is likely that some oleic acid remains anchored on the nanoparticles. The presence of leftover oleic acid cannot be directly observed, and as such we cannot offer that there is, in actuality, no remnant oleic acid remaining on the surface. TEM analysis indicates that the resulting water-soluble nanoparticles have similar polydispersity (± 1.2 – 1.4 nm) as the original oleic acid coated magnetite (Figure 8, Table 1) and are a little smaller than those refunctionalized according to the stripping protocol. Regardless of the hydrophilic ligand used, refunctionalization via the biphasic procedure yields more monodisperse nanoparticles than the stripping procedure (Figure 8). For instance, dopamide-PEG-MION nanoparticles synthesized from the biphasic protocol (Figure 1d) are more uniform than those synthesized according to the stripping protocol (Figure 1c). Furthermore, XRD analysis indicates that nanoparticles refunctionalized according to the biphasic procedure have lattice parameters consistent with magnetite (Table 1).

Magnetism and Relaxivity of Refunctionalized Nanoparticles

In order to investigate the effect of the refunctionalization protocol on the magnetism and the relaxivity of the iron oxide nanoparticles, hysteresis loops and ZFC/FC magnetization were measured for the samples obtained from the biphasic protocol. Unfortunately, the stripping protocol does not yield enough material to enable their magnetic characterization, thereby underlining an important limitation and disadvantage of this procedure over the biphasic protocol. The relaxivity of each sample, functionalized according to both the stripping and the biphasic procedure, were also measured. Importantly, all relaxivity measurements discussed below are the average of three independently synthesized batches of refunctionalized MION. The standard deviation between each identically prepared sample is given in parentheses. Moreover, each refunctionalized hydrophilic MION described below were prepared from the *same batch* of oleic acid coated magnetite nanoparticles. Since each sample was prepared from the same "parent" ferrofluid, the changes described below result solely from the refunctionalization procedure and from the organic coating, and not from minor changes in starting material resulting from two different syntheses of oleic-acid coated nanoparticles precursor.

The magnetic characterization of the iron oxide nanoparticles before and after refunctionalization is given in Table 2. These characterizations include the parameters saturation magnetization (M_S), magnetic coercivity (H_C), remnant magnetization (M_R), blocking temperature (T_B) and transverse relaxivity (r_2). Importantly, the saturation magnetization value are given after extraction of the weight contribution of the organic part. As is apparent from the data, refunctionalizing the nanoparticles has a significant impact both on their magnetic behavior and their efficacy as MRI contrast agents (as measured by relaxivity). Furthermore, both the nature of the anchoring group of the organic coating, and the protocol followed for their refunctionalization impact the magnetism and relaxivity of the nanoparticles. Moreover, to reduce dipolar interactions between particles, the magnetic data of PEG modified nanoparticles was obtained from frozen dispersions of the particles.

The oleic acid coated iron oxide nanoparticles have a mean size of 7.1 ± 1.4 nm and exhibit a saturation magnetization of 49 Am^2/kg. The lower M_S as compared to bulk magnetite (M_S = 87 – 92 Am^2/kg) is likely due to the smaller size of the nanoparticles. Previous studies have indeed reported a decrease in M_S of magnetite with decreasing particle size (1,30). Interestingly, the soap-covered nanoparticles exhibit a saturation magnetization of 71 Am^2/kg, which is 45% larger than that of the hydrophobic oleic acid coated nanoparticles. Notably, this increase in magnetization does not result from an increase in particle size. TEM analysis indicates that the nanoparticles maintain a size of 7.4 ± 1.9 nm. The M_R/M_S ratio also increases compared to the oleic acid coated nanoparticles, suggesting that the positively charged hydrophilic nanoparticles interact even less than their hydrophobic precursor. In comparison, completely non-interacting nanoparticles are predicted to have a M_R/M_S ratio of 0.5 (31,32).

Refunctionalization of the magnetite nanoparticles with PEG ligands affects both the magnetization and the relaxivity of the material. Stripping the nanoparticles result in a significant decrease in saturation magnetization and a significant increase in the blocking temperature. The M_S of the stripped nanoparticles is 59% lower than that of the oleic acid coated precursor, while the blocking temperature doubles to 71 K. Furthermore, TEM analysis (Figure 1b and Table 1) indicates that the particles become more polydisperse, which coincides with a broadening of the ZFC curve. This decrease in magnetization can be somewhat recovered upon refunctionalizing the nanoparticles with PEGs incorporating catechol-type anchors, such as catecholamide or 2,3-dihydroxybenzamide. The relaxivity of the DHB-PEG-MION and dopamide-PEG-MION, although lower than that of the soap covered nanoparticles, remains high, between 70 – 100 $mM_{Fe}^{-1}s^{-1}$. In comparison, the

commercial dextran-based USPIO Sinerem® (Guerbet) has a significantly lower transverse relaxivity of 53 $mM_{Fe}^{-1}s^{-1}$. Notably, refunctionalization with a PEG that contains a different anchoring group, such as phosphonate or carboxylate, does not enable the recovery of the magnetization. PO_3-PEG-MION and CO_2-PEG-MION exhibit transverse relaxivities barely 6 % and 25 % of that of the soap covered nanoparticles. The reason why certain anchoring groups affect the relaxivity of MIONs more than others is not understood, but likely involves either partial oxidation of the surface of the magnetite nanoparticles and/or a difference in spin canting of the surface iron induced by the anchoring group. By measuring the PEG modified nanoparticles from frozen dispersions, the effects of dipolar interactions are reduced, and interpretation of the observed changes in M_s, T_B, and other magnetic variables can be attributed to resulting from changes induced to the surface of the particles.

Refunctionalization of the oleic-acid covered magnetite nanoparticles according to the direct, biphasic protocol yields water-soluble material with much more favorable properties than those obtained by the stripping protocol. MIONs refunctionalized via the biphasic protocol exhibit saturation magnetization similar to the precursor oleic-acid coated nanoparticles. Dopamide-PEG-MION exhibits a M_S slightly lower than that of oleic acid-MION, whereas PO_3-PEG-MION has a slightly higher one. The blocking temperature is also affected by the refunctionalization: T_B of DHB-PEG-MION and dopamide-PEG-MION increase 13 K and 18 K compared to their precursor, respectively. The lower blocking temperature of PO_3-PEG-MION is consistent with the smaller size of the nanoparticles. The change in saturation magnetization upon refunctionalization is translated into the transverse relaxivities of the MIONs. DHB-PEG-MION, dopamide-PEG-MION and PO_3-PEG-MION exhibit relaxivities between 79 and 110 $mM_{Fe}^{-1}s^{-1}$ (Figure 9), which although lower that the soap covered MION, is significantly higher than the commercial USPIO Sinerem®.

Three noteworthy conclusions can be drawn from this study. First, the biphasic procedure for refunctionalization tends to yield nanoparticles of smaller size and higher monodispersity than those obtained from the stripping protocol. Second, catechol-type anchors such as dopamide-PEG and 2,3-dihydroxybenzamide yield material with higher relaxivities. Thirdly, and importantly, refunctionalization according to the biphasic protocol yields nanoparticles with higher relaxivity than comparable ones obtained by the stripping protocol.

The detrimental effect of some anchoring functionalities on the saturation magnetization of iron oxide nanoparticles has already been reported. Herea and coworkers previously reported that the magnetization of iron oxide nanoparticles decreases with increasing ratio of silane coating (33). Gedanken observed that a phosphonic acid coating on Fe_2O_3 nanoparticles severely decreases their magnetization. He suggested that the spin state of surface Fe^{3+} ions was affected by the bonded surfactant, possibly through interaction between the d orbitals of the metal and the p and d orbitals of the anchor (19). Begin-Colin also observed a significant decrease in the M_s of magnetite coated with carboxylates, but no decrease in magnetization with organic coating bearing phosphonate anchors (34). The apparent contradiction between the result of Begin-Colin and that of Gedanken could be explained in light of our results. For phosphonate coating, the protocol followed for the refunctionalization of the iron oxide nanoparticles seems to have a significant impact on the resulting magnetic behavior of the material. Refunctionalization with phosphonate ligands according to the biphasic procedure yields material with high relaxivity, whereas functionalization according to the two-step, stripping procedure significantly decreases the relaxivity of the particles. Significantly, our study not only systematically demonstrates the different impact of different anchoring functionalities on the magnetic properties of magnetite nanoparticles, but also translates these results to the application of these materials as contrast agents for medical MRI.

Reaction of Dopamine with Iron Oxide Nanoparticles

Dopamine was previously reported to react with Fe(III) according to a radical mechanism to produce leucodopaminochrome (35). More recently, the decomposition of dopamine was also reported to occur in the presence of iron oxide nanoparticles (24). Accordingly, and in light of the above results, we postulated that the magnetic behavior of the iron oxide nanoparticles would be significantly affected by this surface reaction. Refunctionalization of oleic acid coated magnetite with dopamine according to the biphasic procedure significantly decreases the size of the particles. The FT-IR spectrum of dopamine-MION is significantly different than that of dopamine (Figure 2 n and o). These observations, together with the blue color of the ferrofluid (all other nanoparticles suspensions are dark brown) indicate that the dopamine coating reacts with the magnetite nanoparticles. Our observations are thus in agreement with those reported by Carpenter (24).

Notably, the decomposition of dopamine also has a significant impact on the structure and magnetic behavior of the resulting nanomaterial. XRD analysis (Figure 3e) indicates that the iron oxide nanoparticles are no longer composed of pure magnetite or maghemite. A number of peaks that do not correspond to either phase are now also present. While it is uncertain what the composition of the final material is, the impact of this reaction on its magnetic behavior is significant. The blocking temperature of the material increases from 34 K to 82 K (Figure 4). Importantly, the reaction of dopamine with the magnetite nanoparticles significantly decreases both their longitudinal (r_1) and transverse (r_2) relaxivities. The r_2 of the dopamine-MION reaction product (16 $mM_{Fe}^{-1}s^{-1}$) is only 12 % that of the soap covered magnetite (130 $mM_{Fe}^{-1}s^{-1}$). A similar decrease in r_1 upon reaction with dopamine is observed, particularly at low magnetic fields (Figure 10). Interestingly, a bigger change in the blocking temperature and in relaxivity is observed when the refunctionalization is performed according to the biphasic procedure, which further underlines the influence of the functionalization protocol on the properties of the final material.

The significant effects of the dopamine functionalization suggest that after coordination of surface iron, the dopamine likely reacts via a radical mechanism involving both a semiquinone and a quinine intermediates to form leucodopaminochrome (35). This reaction largely decomposes the magnetite core, likely through a process which involves reduction of Fe(III) to Fe(II), thereby changing the phase and partially dissolving the surface of the nanoparticles.

Notably, this reaction no longer occurs when the amine group of dopamine is altered to an amide group. The dopamide-PEG presented beforehand stabilizes the nanoparticles effectively, and do not appear to change the phase nor to dissolve the magnetite core. The resulting pegylated particles present high transverse relaxivity (110 $mM_{Fe}^{-1}s^{-1}$). The increased stability of dopamide-PEG could potentially result from coordination of the iron from the amide moiety. Moreover, it is unlikely that the quinine intermediate could react with a protonated amide to form an indole ring, as is the case in the reaction of dopamine. Comparison of dopamine and dopamide-PEG indicate how a simple change in the functionality of the anchoring group can have a significant impact on the magnetic property of the resulting material.

Conclusions

This study highlights the significant impact of the organic coating on the magnetic properties and relaxivity of iron oxide nanoparticles used as contrast agents for medical magnetic resonance imaging. Specifically, two parameters were found to influence relaxivity: the anchoring group and the refunctionalization protocol. Anchoring groups that contain catechol functionalities, such as dopamide and 2,3-dihydroxybenzamide were found

to retain most efficiently the relaxivity and saturation magnetization of the oleic-acid coated magnetite precursors. Other groups, such as carboxylate and especially dopamine alone, significantly decrease the relaxivity of the magnetite, either by reacting with the nanoparticles, or possibly, by altering the spin canting of the irons. The protocol followed for the refunctionalization was also found to have a significant impact on the relaxivity of the nanoparticles. In each case, for a given PEG, the relaxivity obtained for magnetite nanoparticles refunctionalized according to the biphasic protocol is higher than that of material obtained from the stripping protocol. The influence of the organic coating on the magnetic behavior and relaxivity of iron oxide nanoparticles should therefore not be ignored. The choice of the anchoring functionality and refunctionalization protocol are parameters crucial to the behavior of the material which should be taken into consideration when synthesizing particulate contrast agents for MRI.

Supplementary Material

Refer to Web version on PubMed Central for supplementary material.

Acknowledgments

This work was supported by the Chemistry-Biology Interface Training Grant from the National Institutes of Health, and the University of Minnesota, Twin-Cities. Parts of this work were carried out in the Institute of Technology Characterization Facility, University of Minnesota, a member of the NSF-funded Materials Research Facilities Network (www.mrfn.org). The low temperature magnetic measurements were performed at the Institute for Rock Magnetism (IRM) at University of Minnesota. IRM is funded by the Instrumentation and Facilities program of the Earth Science Division of National Science Foundation (NSF), W. M. Keck Foundation and the University of Minnesota. This is IRM contribution # 0907. We thank Prof. Lee Penn (Department of Chemistry, University of Minnesota) for the use of the X-Ray Diffractometer. We thank Prof. Silvio Aime, University of Turin, Italy, for the use of the fast-field cycling relaxometer to measure the NMRD profile.

REFERENCES

1. Cheon J, Lee J-H. Synergistically integrated nanoparticles as multimodal probes for nanobiotechnology. Acc. Chem. Res. 2008; 41:1630–1640.
2. Di Marco M, Sadun C, Port M, Guilbert I, Couvreur P, Dubernet C. Physicochemical characterization of ultrasmall superparamagnetic iron oxide particles (USPIO) for biomedical application as MRI contrast agents. Int. J. Nanomedicine. 2007; 2:609–622. [PubMed: 18203428]
3. Laurent S, Forge D, Port M, Roch A, Robic C, Vander Elst L, Muller RN. Magnetic iron oxide nanoparticles: Synthesis, stabilization, vectorization, physicochemical characterizations, and biological applications. Chem. Rev. 2008; 108:2064–2110. [PubMed: 18543879]
4. Muller, RN.; Roch, A.; Colet, J-M.; Ouakssim, A.; Gillis, P. Particulate magnetic contrast agents. In: Merbach, AE.; Tóth, E., editors. The chemistry of contrast agents. Chichester: Wiley; 2001.
5. Jung CW, Jacobs P. Physical and chemical-properties of superparamagnetic iron-oxide mr contrast agents - ferumoxides, ferumoxtran, ferumoxsil. Magn. Reson. Imaging. 1995; 13:661–674. [PubMed: 8569441]
6. Powell DH, NiDhubhghaill OM, Pubanz D, Helm L, Lebedev YS, Schlaepfer W, Merbach AE. Structural and dynamic parameters obtained from O-17 NMR, EPR, and NMRD studies of monomeric and dimeric Gd^{3+} complexes of interest in magnetic resonance imaging: An integrated and theoretically self consistent approach. J. Am. Chem. Soc. 1996; 118:9333–9346.
7. Toth E, Helm L, Merbach AE. Relaxivity of MRI contrast agents. Top. Curr. Chem. 2002; 221:61–101.
8. Caravan P, Ellison JJ, McMurry TJ, Lauffer RB. Gadolinium(III) chelates as MRI contrast agents: Structure, dynamics, and applications. Chem. Rev. 1999; 99:2293–2352. [PubMed: 11749483]
9. Geraldes CFGC, Laurent S. Classification and basic properties of contrast agents for magnetic resonance imaging. Contrast Media Mol. Imaging. 2009; 4:1–23. [PubMed: 19156706]

10. Chan KWY, Wong WT. Small molecular gadolinium(III) complexes as MRI contrast agents for diagnostic imaging. Coord. Chem. Rev. 2007; 251:2428–2451.
11. Roch A, Muller RN, Gillis P. Theory of proton relaxation induced by superparamagnetic particles. J. Chem. Phys. 1999; 110:5403–5411.
12. Ouakssim A, Fastrez S, Roch A, Laurent S, Gossuin Y, Piérart C, Vander Elst L, Muller RN. Control of the synthesis of magnetic fluids by relaxometry and magnetometry. J. Magn. Magn. Mater. 2004; 272–276:E1711–E1713.
13. Roch A, Gillis P, Ouakssim A, Muller RN. Proton magnetic relaxation in superparamagnetic aqueous colloids: A new tool for the investigation of ferrite crystal anisotropy. J. Magn. Magn. Mater. 1999; 201:77–79.
14. Bulte JWM, Brooks RA, Moskowitz BM, Henry Bryant JL, Frank JA. T1 and t2 relaxometry of monocrystalline iron oxide nanoparticles (MION-46L): Theory and experiment. Acad. Radiol. 1998; 5:S137–S140. [PubMed: 9561064]
15. Roch A, Muller RN, Gillis P. Water relaxation by spm particles: Neglecting the magnetic anisotropy? A caveat. J. Magn. Reson. Imaging. 2001; 14:94–96. [PubMed: 11436221]
16. Park J, An K, Hwang Y, Park J-G, Noh H-J, Kim J-Y, Park J-H, Hwang N-M, Hyeon T. Ultra-large-scale syntheses of monodisperse nanocrystals. Nat. Mater. 2004; 3:891–895. [PubMed: 15568032]
17. Morales MP, Veintemillas-Verdaguer S, Montero MI, Serna CJ, Roig A, Casas L, Martinez B, Sandiumenge F. Surface and internal spin canting in γ-Fe_2O_3 nanoparticles. Chem. Mater. 1999; 11:3058–3064.
18. Wu W, He QG, Jiang CZ. Magnetic iron oxide nanoparticles: Synthesis and surface functionalization strategies. Nano. Res. Lett. 2008; 3:397–415.
19. Yee C, Kataby G, Ulman A, Prozorov T, White H, King A, Rafailovich M, Sokolov J, Gedanken A. Self-assembled monolayers of alkanesulfonic and -phosphonic acids on amorphous iron oxide nanoparticles. Langmuir. 1999; 15:7111–7115.
20. Sahoo Y, Pizem H, Fried T, Golodnitsky D, Burstein L, Sukenik CN, Markovich G. Alkyl phosphonate/phosphate coating on magnetite nanoparticles: A comparison with fatty acids. Langmuir. 2001; 17:7907–7911.
21. Daou TJ, Grenèche JM, Pourroy G, Buathong S, Derory A, Ulhaq-Bouillet C, Donnio B, Guillon D, Begin-Colin S. Coupling agent effect on magnetic properties of functionalized magnetite-based nanoparticles. Chem. Mater. 2008; 20:5869–5875.
22. Herea DD, Chiriac H. One-step preparation and surface activation of magnetic iron oxide nanoparticles for bio-medical applications. Optoelectron. and Adv. Mat. 2008; 2:549–552.
23. Xu C, Xu K, Gu H, Zheng R, Liu H, Zhang X, Guo Z, Xu B. Dopamine as a robust anchor to immobilize functional molecules on the iron oxide shell of magnetic nanoparticles. J. Am. Chem. Soc. 2004; 126:9938–9939. [PubMed: 15303865]
24. Shultz MD, Reveles JU, Khanna SN, Carpenter EE. Reactive nature of dopamine as a surface functionalization agent in iron oxide nanoparticles. J. Am. Chem. Soc. 2007; 129:2482–2487. [PubMed: 17290990]
25. Sun SH, Zeng H, Robinson DB, Raoux S, Rice PM, Wang SX, Li GX. Monodisperse MFe_2O_4 (M = Fe, Co, Mn) nanoparticles. J. Am. Chem. Soc. 2004; 126:273–279. [PubMed: 14709092]
26. Martínez-Mera I, Espinosa-Pesqueira ME, Pérez-Hernández R, Arenas-Alatorre J. Synthesis of magnetite (Fe_3O_4) nanoparticles without surfactants at room temperature. Mater. Lett. 2007; 61:4447–4451.
27. Balasubramanian S, Xuefei H. Functionalization of magnetic nanoparticles with organic molecules: Loading level determination and evaluation of linker length effect on immobilization. Chirality. 2008; 20:265–277. [PubMed: 17568438]
28. Patterson AL. The Scherrer formula for X-ray particle size determination. Phys. Rev. 1939; 56:978–982.
29. Weissleder R, Elizondo G, Wittenberg J, Rabito CA, Bengele HH, Josephson L. Ultrasmall superparamagnetic iron-oxide - characterization of a new class of contrast agents for mr imaging. Radiology. 1990; 175:489–493. [PubMed: 2326474]

30. Young-wook J, Jae-Hyun L, Jinwoo C. Chemical design of nanoparticle probes for high-performance magnetic resonance imaging. Angew. Chem., Int. Ed. Engl. 2008; 47:5122–5135. [PubMed: 18574805]

31. Goya GF, Berquo TS, Fonseca FC, Morales MP. Static and dynamic magnetic properties of spherical magnetite nanoparticles. J. Appl. Phys. 2003; 94:3520–3528.

32. Hadjipanayis G, Sellmyer DJ, Brandt B. Rare-earth rich metallic glasses .1. Magnetic hysteresis. J. Phys. Rev. B. 1981; 23:3349–3354.

33. Herea DD, Chiriac H. One-step preparation and surface activation of magnetic iron oxide nanoparticles for bio-medical applications. Optoelectronics Adv. Mat. 2008; 2:549–552.

34. Daou TJ, Grenèche JM, Pourroy G, Buathong S, Derory A, Ulhaq-Bouillet C, Donnio B, Guillon D, Begin-Colin S. Coupling agent effect on magnetic properties of functionalized magnetite-based nanoparticles. Chem. Mater. 2008; 20:5869–5875.

35. El Ayaan U, Herlinger E, Jameson RF, Linert W. Anaerobic oxidation of dopamine by iron(III). J. Chem. Soc., Dalton Trans. 1997:2813–2818.

36. Rohrer M, Bauer H, Mintorovitch J, Requardt M, Weinmann H-J. Comparison of Magnetic Properties of MRI Contrast Media Solutions at Different Magnetic Field Strengths. Investigative Radiol. 2005; 40:715–724.

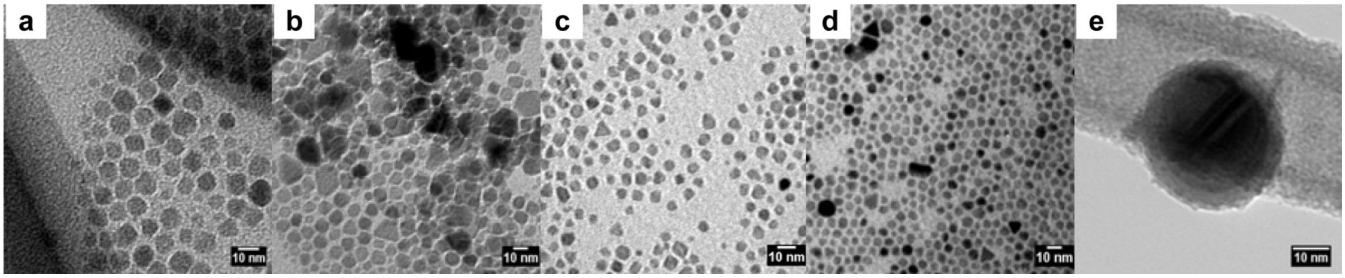

Figure 1.
TEM images of a) oleic acid-MION, b) stripped-MION, c) Dopamine-PEG-MION synthesized by direct ligand exchange, d) Dopamine-PEG-MION synthesized according to the stripping protocol, and e) dopamine-MION.

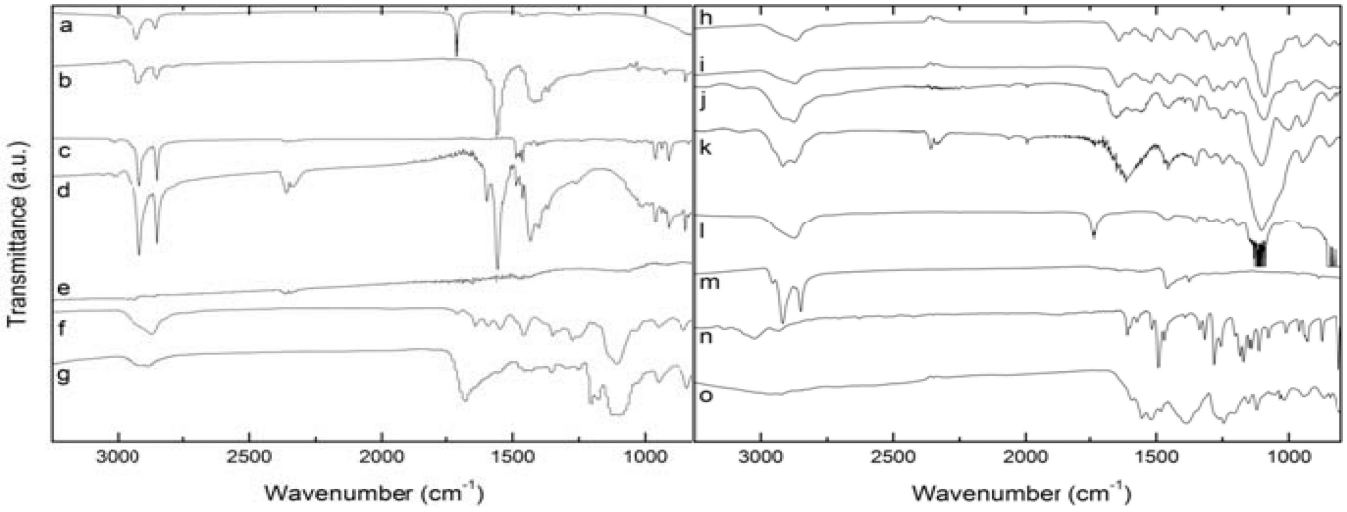

Figure 2.

IR spectra of a) oleic acid, b) oleic acid-MION, c) soap, d) oleic acid-soap-MION, e) stripped-MION, f) DHB-PEG, g) DHB-PEG-MION, h) dopamide-PEG, i) dopamide-PEG-MION, j) PO_3-PEG, k) PO_3-PEG-MION, l) CO_2-PEG, m) CO_2-PEG-MION, n) dopamine, and o) dopamine-MION.

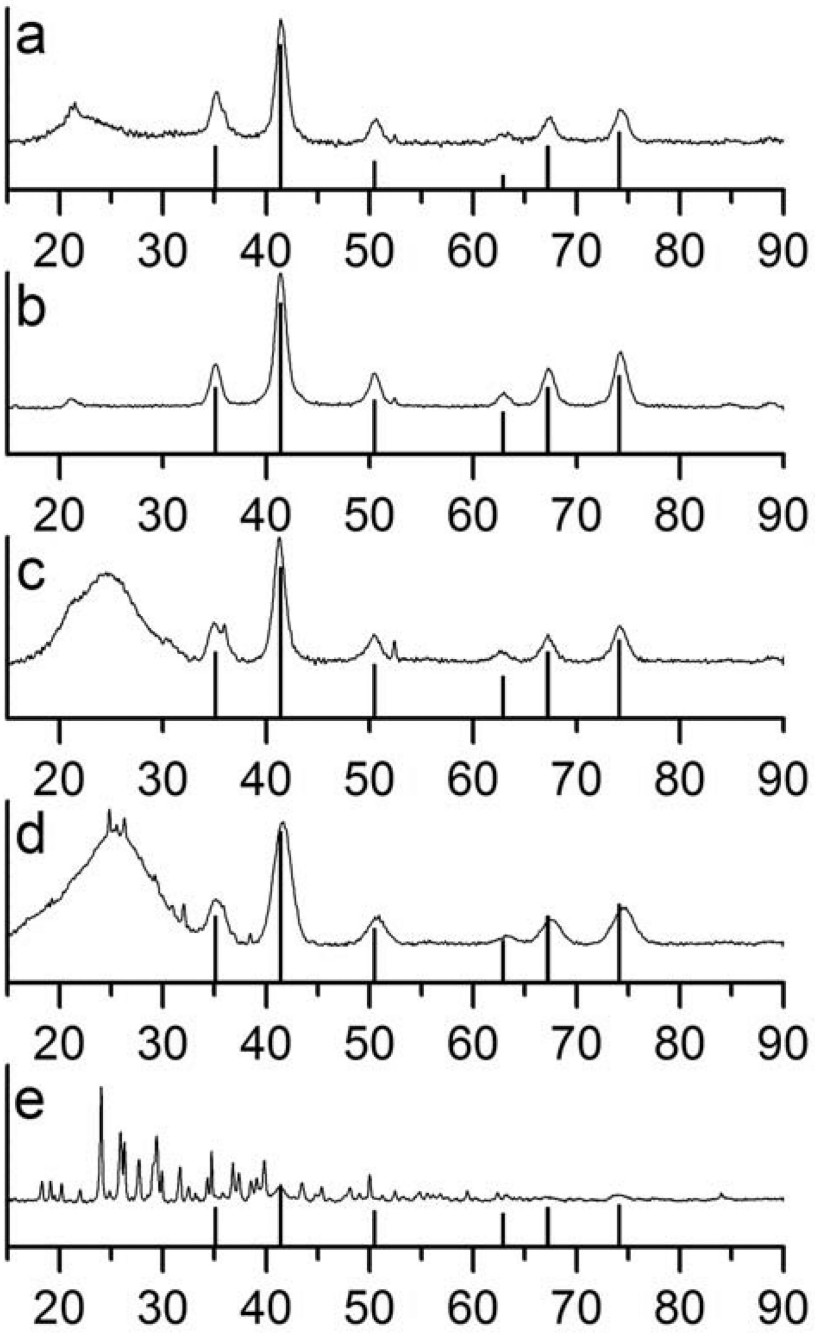

Figure 3.
X-ray diffraction patterns of a) oleic acid-MION, b) stripped-MION, and surface-functionalized MION synthesized according to the biphasic protocol: c) dopamide-PEG-MION, d) PO_3-PEG-MION and e) dopamine-MION.

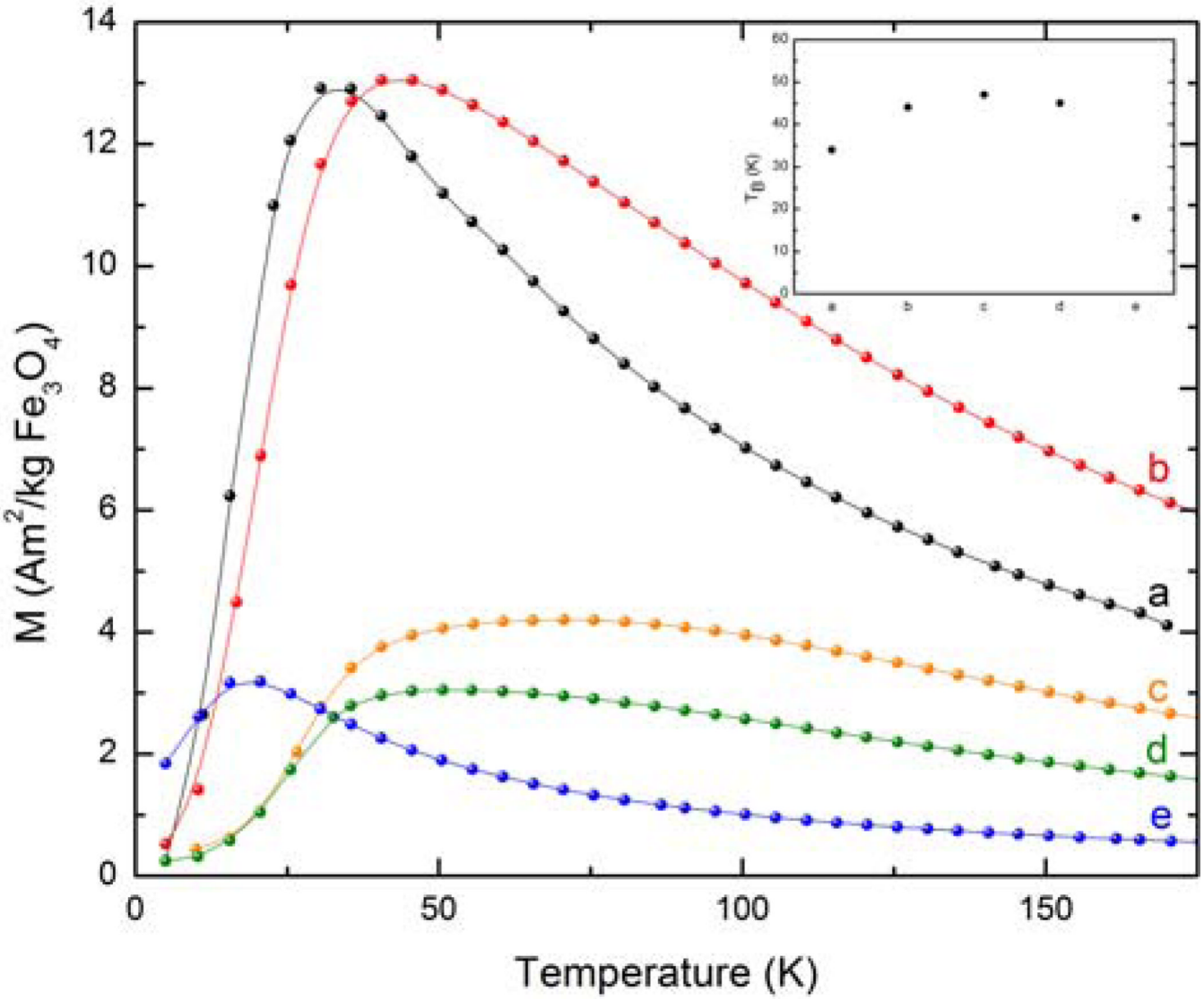

Figure 4.
ZFC curves of a) oleic acid-MION, b) oleic acid-soap-MION, c) stripped-MION, d) dopamide-PEG-MION, and e) PO_3-PEG-MION. Note: curves c and d represent MIONs functionalized via the biphasic protocol.

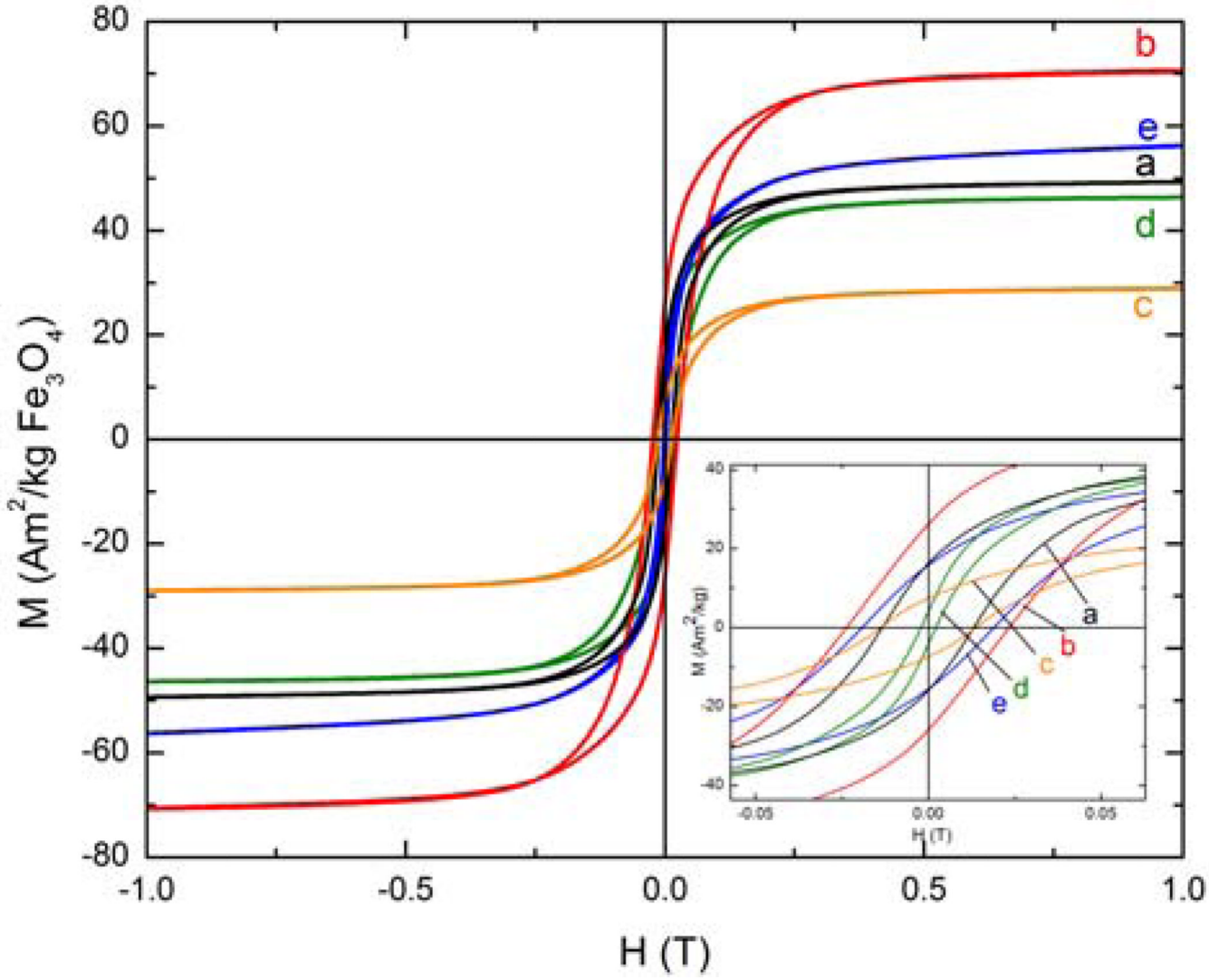

Figure 5.
Hysteresis loops of a) oleic acid-MION, b) oleic acid-soap-MION, c) stripped-MION, d) dopamide-PEG-MION, and e) PO_3-PEG-MION. Note: curves c and d represent MIONs functionalized via the biphasic protocol.

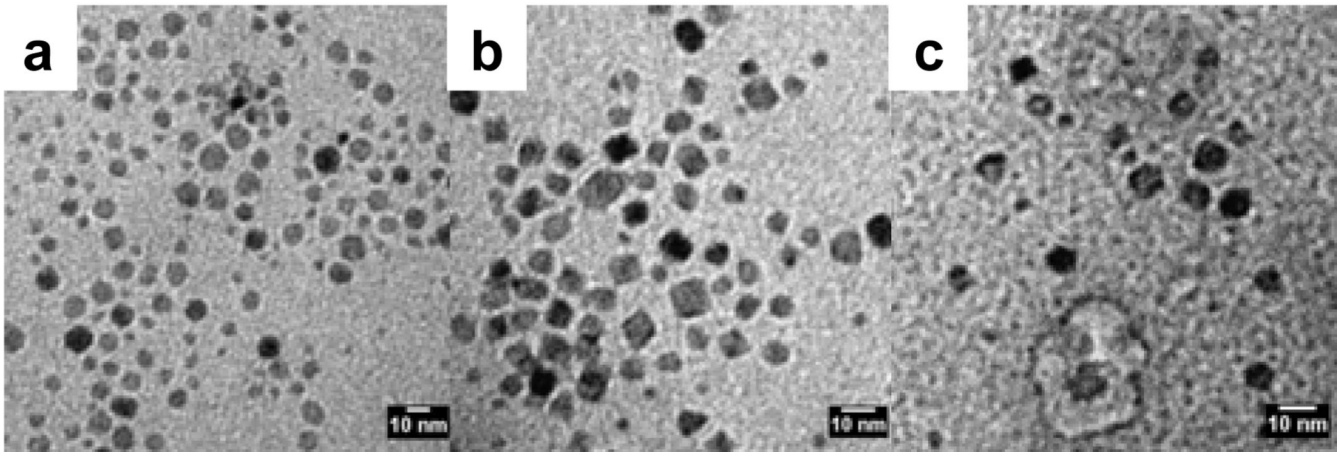

Figure 6.
TEM images of surface functionalized MION synthesized according to the stripping protocol: a) DHB-PEG-MION, b) PO_3-PEG-MION, and c) CO_2-PEG-MION.

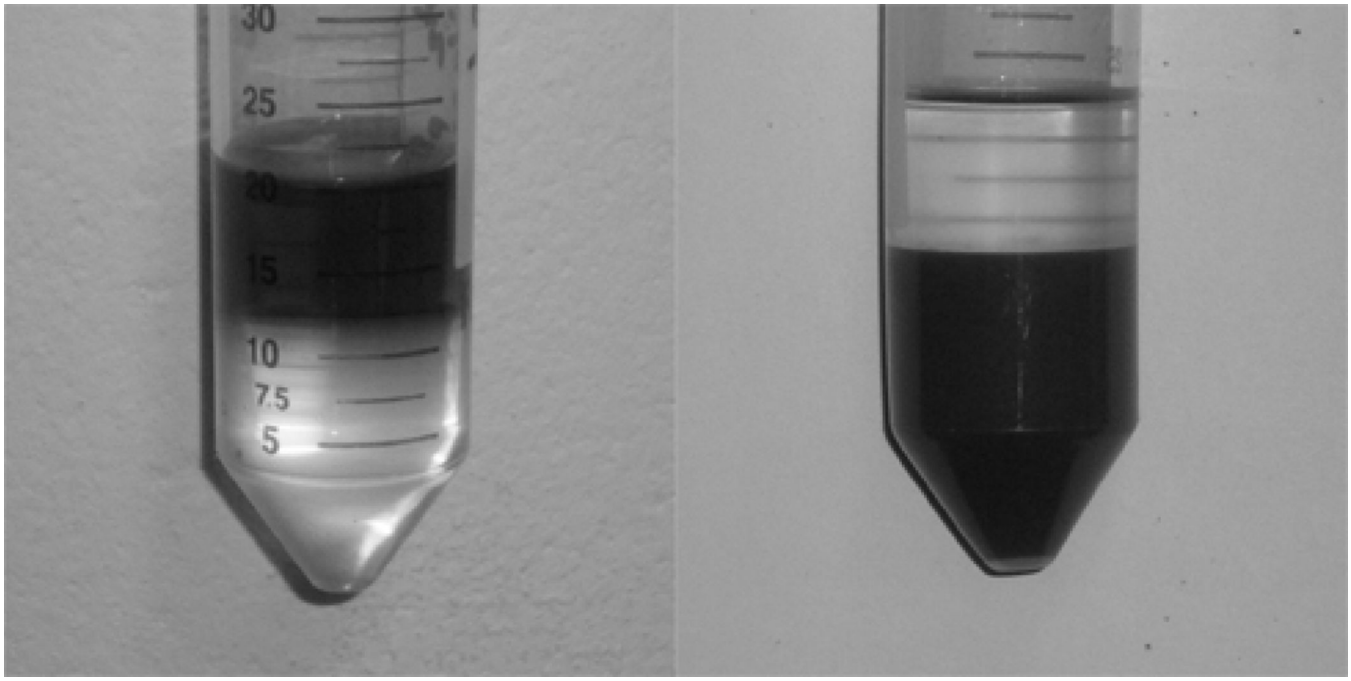

Figure 7.
Typical refunctionalitazation effects to create water dispersible nanoparticles (illustrated in Scheme 1). Initially, the oleic acid stabilized nanoparticles are dispersed in the hexanes phase of a hexane/water mixture (left). After functionalization with water-amenable ligands, the nanoparticles transfer into the aqueous phase and are no longer stabilized by hexanes (right).

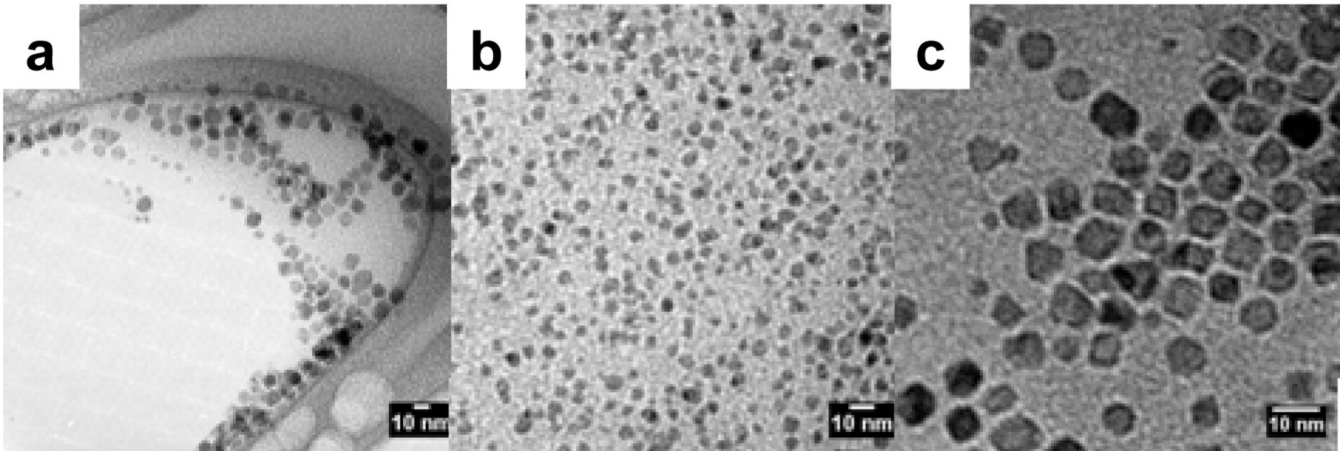

Figure 8.
TEM images of surface-functionalized MION synthesized by direct ligand exchange: a) oleic acid-soap-MION, b) DHB-PEG-MION, and c) PO_3-PEG-MION.

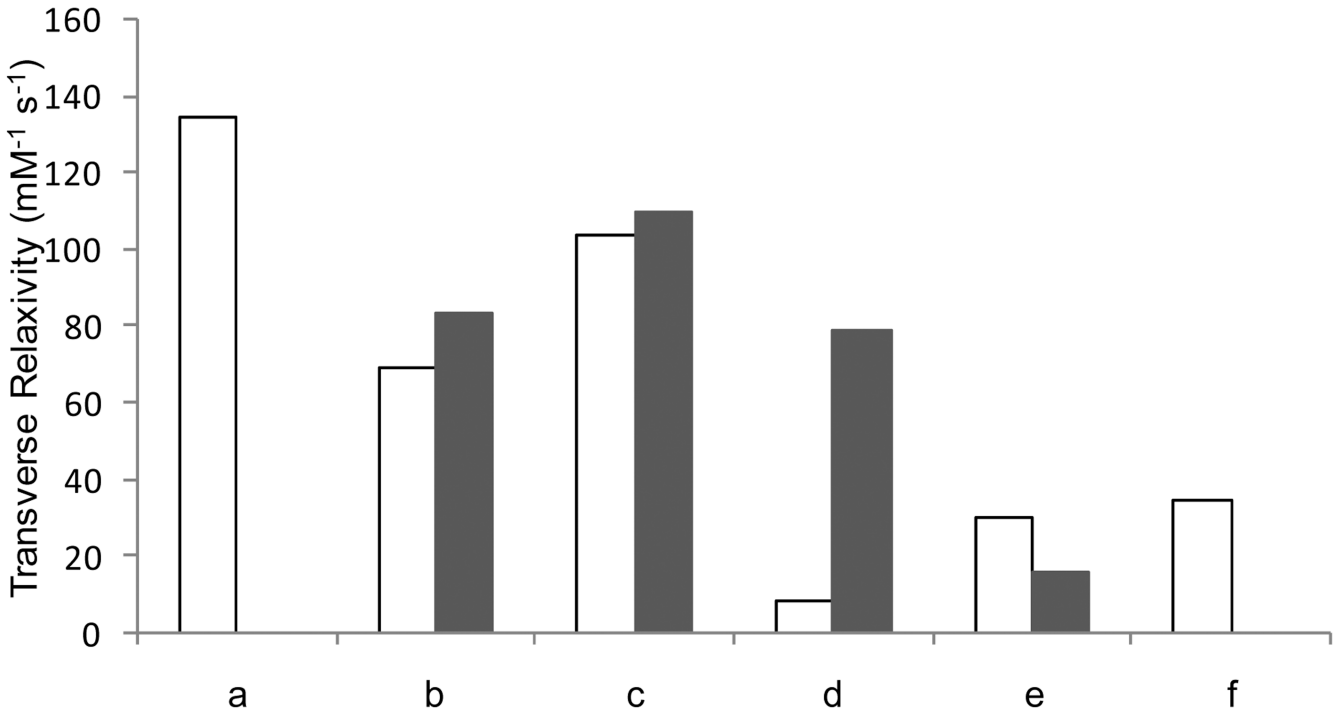

Figure 9.

Transverse relaxivity of a) oleic acid-soap-MION, b) DHB-PEG-MION, c) dopamide-PEG-MION, d) dopamine-MION, and e) PO_3-PEG-MION, and f) CO_2-PEG-MION. White bars represent nanoparticles functionalized according to the stripping protocol. Black bars represent nanoparticles functionalized according to the direct, biphasic protocol.

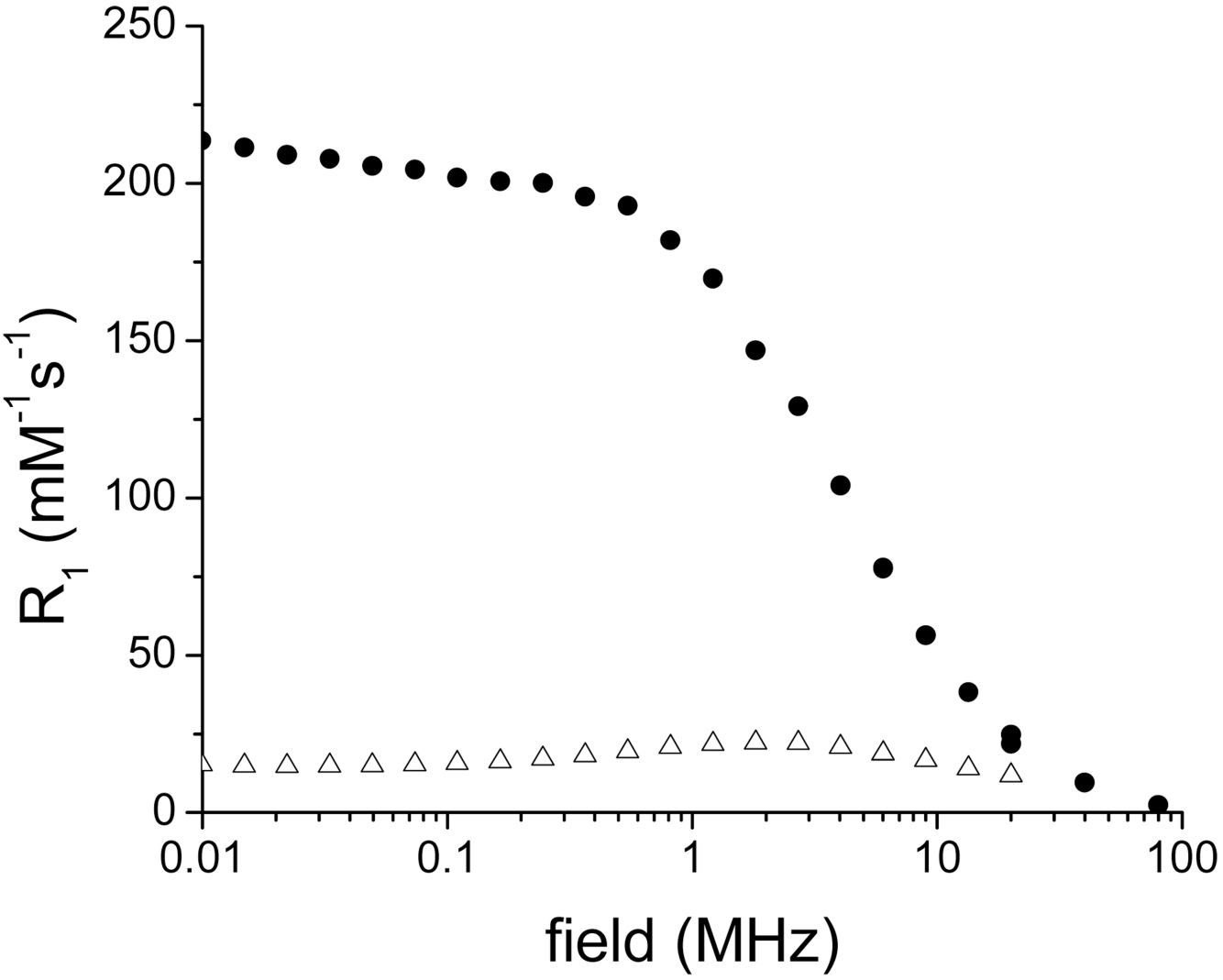

Figure 10.
NMRD profile of oleic acid-soap-MION (filled circle) and dopamine-MION (open triangles).

Table 1

Average particle diameters and polydispersity extracted from TEM and powder XRD, and lattice parameters of iron oxide crystals before and after functionalization.

Sample	Protocol	Core size (nm) (TEM)	Polydispersity (nm) (TEM)	Crystal size (nm) (XRD)	Lattice Parameters (XRD)
Oleic-acid-MION	-	7.1	1.4	8.6	8.40(2)
Oleic acid-soap-MION	-	7.6	1.9	-	8.36(3)
Stripped MION	a	7.0	2.0	8.6	8.38(2)
DHB-PEG-MION	a	6.9	1.2	-	-
	b	7.0	1.2	7.2	-
Dopamide-PEG-MION	a	7.4	2.1	-	-
	b	6.7	1.2	8.0	8.40(2)
PO_3-PEG-MION	a	6.6	2.0	-	-
	b	5.5	1.0	4.4	8.41(3)
CO_2-PEG-MION	a	7.3	1.4	-	-
Dopamine MION	a	7.56	1.2	-	-
	b	6.6	1.4	-	-
Sinerem®	c	4.9	1.5	6.0	8.37(2)

a) stripping of surface-bound oleic acid with ethanol followed by coordination of ligand,

b) direct ligand exchange in a biphasic system,

c) data from reference 5.

Table 2

Relaxivities and magnetic characterization of surface-functionalized MION.

Sample	Protocol	r_2 ($mM^{-1}s^{-1}$)	M_S (Am^2/kg)	H_c [e] (T)	M_R/M_S [e]	T_B (K)
Oleic acid-MION	-	*c*	49	0.013	0.33	34
Oleic acid-soap-MION	-	134(3)	71	0.023	0.38	44
Stripped MION	a	*c*	29	0.014	0.26	71
Dopamide-PEG-MION	a	103(2)	-	-	-	-
	b	110(3)	46	0.020	0.34	52
DHB-PEG-MION	a	69.4(3)	-	-	-	-
	b	83.8(3)	-	-	-	47
PO_3-PEG-MION	a	8.2(2)	-	-	-	-
	b	79(3)	56	0.0021	0.078	18
CO_2-PEG-MION	a	35(3)	-	-	-	45
Dopamine-MION	a	30(6)	-	-	-	77
	b	16(2)	-	-	-	82
Sinerem®	d	53.1	94.8	-	-	60

[a] Stripping of surface-bound oleic acid with ethanol followed by coordination of ligand,

[b] direct ligand exchange in a biphasic system,

[c] not water soluble,

[d] data from Reference 5,

[e] measured at 10 K. R_2 = transverse relaxivity at 300 MHz, M_S = saturation magnetization, H_C = coercive field, M_R = remanence, T_B = blocking temperature. Numbers in parentheses indicate standard deviation from three different samples and synthetic batches.